Land plant evolution and volcanism led to the Late Devonian mass extinction

Matthew Smart (✉ smartm@iu.edu)

United States Naval Academy   https://orcid.org/0000-0002-9330-0381

Gabriel Filippelli

Indiana University   https://orcid.org/0000-0003-3434-5982

William Gilhooly III

Indiana University-Purdue University, Indianapolis   https://orcid.org/0000-0002-5931-5571

Kazumi Ozaki

Tokyo Institute of Technology

Christopher Reinhard

Georgia Institute of Technology   https://orcid.org/0000-0002-2632-1027

John Marshall

University of Southampton   https://orcid.org/0000-0002-9242-3646

Jessica Whiteside

University of Southampton

Version of Record: A version of this preprint was published at Communications Earth & Environment on November 29th, 2023. See the published version at https://doi.org/10.1038/s43247-023-01087-8.

Abstract

The evolution of land plants in terrestrial environments brought about one of the most dramatic shifts in the history of the Earth system — the birth of modern soils — and likely stimulated massive changes in marine biogeochemistry and climate. In particular, multiple marine mass extinctions characterized by widespread anoxia, including the Late Devonian mass extinction around 375 million years ago (Ma), may have been linked to terrestrial nutrient release driven by newly-rooted landscapes. Here, we use recently generated constraints from Earth's lacustrine rock record as variable inputs in an Earth system model of the coupled C-N-P-O_2-S biogeochemical cycles in order to evaluate whether recorded changes to phosphorus fluxes would be adequate to sustain Devonian marine biogeochemical perturbations and extinction dynamics. Results show that globally scaled riverine phosphorus export during the Late Devonian mass extinction generates widespread marine anoxia and produces carbon isotope, temperature, oxygen, and carbon dioxide perturbations generally consistent with the geologic record. Similar results for a competing extinction mechanism, large scale volcanism, suggest the Late Devonian mass extinction was likely multifaceted with both land plants and volcanism as contributing factors.

Introduction

The Late Devonian mass extinction (also called the Frasnian-Famennian extinction and alternatively the Kellwasser Event) is one of the "Big Five" Phanerozoic mass extinctions[1,2]. It is characterized by two distinct episodes of widespread marine anoxia[3,4] expressed in the sedimentary record by the deposition of distinct black shale horizons[3-5]. It is largely thought to have occurred in two distinct pulses, the earliest being the Lower Kellwasser (LKW) and the latter the Upper Kellwasser (UKW). Both pulses are associated with significant global carbon cycle perturbations, with positive carbon-isotope excursions ($d^{13}C$) ranging up to 4‰ reported in numerous studies[4-7]. The development of sustained marine anoxia is linked to the demise of bottom-dwelling marine species[3,8,9], and it is also thought that water column oxygen depletion played a direct role in the catastrophic collapse of Devonian reef ecosystems[2,10]. Proposed mechanisms for the Late Devonian extinction include climate perturbations (both warming and cooling[11-15]), astronomical forcing[16,17], bolide impacts[18,19], large igneous province (LIP) eruptions[20,21], enhanced terrestrial weathering associated with mountain building[22,23] and the evolution and expansion of land plants[24-26]. Despite the lack of agreement on a single initiating event, many studies cite nutrient influx either from elevated terrestrial input or marine upwelling as a contributing factor[4,26,27].

Global biogeochemical perturbations associated with the Late Devonian extinction have been widely reported (i.e., global positive $d^{13}C$ excursions). Numerous investigations into the geologic record across the KW events revealed additional global trends which exist independent of extinction ascription, such as the precipitous decline in atmospheric CO_2[28-31], the rise in atmospheric O_2 to near modern levels[31-34] and the overall increase in global average temperature[35]. Given the wealth of information in the geologic record, the question arises as to whether global biogeochemical cycling supports any of these theories

regarding the causal factor (or factors) driving the Late Devonian extinction. This question is particularly relevant as it relates to two diverging theories regarding extinction initiation, large scale volcanism and enhanced terrestrial nutrient export related to land plant evolution and expansion. Three significant LIP eruptions occurred temporally proximal to the KW events (Fig. 1b), suggesting large scale volcanism had some impact on biogeochemical cycling, and may have played a significant role in contemporaneous mass extinction. At the same time, land plant evolution reached a zenith in the Late Devonian as the earliest trees with significant root systems achieved hegemony by the late Famennian[37-39]. These tectonic and biotic events potentially influenced global geochemical cycles in the Devonian, each leaving their own forensic footprint in the geologic record. Here we investigate the global geochemical impact of each of these events by utilizing new proximal continental lacustrine records of phosphorus accumulation rate changes and employing an Earth system box model to simulate the carbon, nitrogen, phosphorus, oxygen and sulfur biogeochemical cycles. We explore both pulses of the Late Devonian extinction to determine which of these two processes, tectonic or biologic, could most plausibly result in the observed geochemical changes recorded in the rock record.

Enhanced Phosphorus Export During the Late Devonian Mass Extinction

The role of land plants in Devonian biotic crises has long been a subject of debate. First suggested by Algeo et al.[24], the theory proposes that the expansion of land plants into continental interiors along with the development of significant root systems and arborescence led to an unprecedented flux of terrestrial nutrients into Devonian seas. The relatively large and rapid nutrient load would have stimulated primary productivity leading to eutrophication, elevated organic matter deposition and subsequent bottom water anoxia. Occurring on a large enough scale, this could drive marine mass extinctions, which were relatively common throughout the Devonian[24]. Until recently however, no studies have focused on quantifying a potential terrestrial nutrient pulse from land plant expansion by interrogating weathering-proximal terrestrial lacustrine records. Smart et al.[26] reported two such pulses in a fluvial sequence in the Devonian Basin of East Greenland associated with the LKW and UKW (Fig. 2). These pulses are directly associated with land plant expansion and were both significant in magnitude and sustained in duration[26], enabling their use in geochemical models. The increases in phosphorus accumulation rates[26] compare favorably to revegetation following glacial retreat in Holocene analogues, lending confidence in the utility of their data (Extended Data Table 1). Furthermore, the paleogeographic location of the Heintzbjerg study site was on the flanks of the Caledonian mountains and within a drainage basin that fed the Rheic Ocean (Fig. 1). Thus, elevated nutrient export from this location likely had a marked impact on the relatively restricted Rheic Ocean, making this site an ideal candidate from which to estimate global phosphorus flux.

Model description

In this study, we employ an Earth system box model of the coupled C-N-P-O_2-S biogeochemical cycles developed by Ozaki and Reinhard[40]. The basic model design is based on the Carbon Oxygen Phosphorus

Sulfur Evolution (COPSE) model[41,42]. The model includes a series of biogeochemical processes operating on the planetary surface but is abstracted enough to allow the simulations on geologic time scales (see *Methods* and *Supplementary Information*).

We conduct several different runs in which we explore biological and tectonic factors individually. First, we explore the possible impacts of enhanced phosphorus weathering by land plant colonization using both P/Al and phosphorus accumulation rate data from Heintzbjerg, Greenland. In the sensitivity experiments, discrete episodes of phosphorus weathering are assumed with different timing and amplitude. Sharp increases followed by decreases of phosphorus weathering are meant to represent possible phases of selective phosphorus weathering associated with land plant colonization and a subsequent drop due to the establishment of phosphorus recycling in soil systems[42]. We also explore the impacts of variations in degassing rates from LIPs that were active during the upper Devonian (Fig. 1b). In this scenario, we simulate two episodes of large-scale volcanism, a smaller event at the onset of the LKW and a larger event at the onset of the UKW.

Results And Discussion

Results for the enhanced terrestrial nutrient export scenario are shown in Fig. 3. Our model demonstrates the increases in riverine phosphorus flux to the ocean promotes oceanic eutrophication and deoxygenation (as shown as increases in DOA, or degree of anoxia). For the LKW, the enhanced burial of organic matter in the ocean leads to a drop in atmospheric CO_2 levels (from ~10.5 present atmospheric level (PAL) to ~7.5-9 PAL) and associated climate cooling of 0.5-1.5°C. This is accompanied with a positive excursion in $d^{13}C$ of 1.5 to 3.0‰. These trends are observed in both the red/blue simulations as well as the scaled P/Al data from Heintzbjerg (black line in Fig. 3). Also observed is that greater phosphorus weathering results in larger environmental changes. In the large linear simulation (blue line in Fig. 3), atmospheric O_2 levels exhibit a stepwise increase to the modern level of 21%. On the other hand, the sulfur isotopic value of seawater sulfate is largely insensitive to the variations of phosphorus weathering. Results based on the phosphorus accumulation rate data are similar, with a notable difference being the much smaller perturbations associated with the LKW.

Results for the enhanced volcanic degassing scenarios are shown in Fig. 4. A two-fold increase in degassing rate produces a positive excursion in $d^{13}C$ (1‰) for the LKW, and a five-fold increase is required to produce the 2‰ excursion for the UKW. Such an enhanced volcanic flux during the UKW results in atmospheric CO_2 levels of >20 PAL and associated >4°C increase in global temperatures. Under such conditions, an enhanced greenhouse accelerates terrestrial phosphorus weathering, promoting oceanic eutrophication and deoxygenation. This, in turn, leads to the enhanced burial of organic matter in marine sediments and a stepwise increase in atmospheric oxygen (O_2).

The terrestrial nutrient export scenarios and volcanic activity scenarios both demonstrate enhanced riverine phosphorus input flux, resulting in similar behaviors with respect to oceanic biogeochemical dynamics (eutrophication, deoxygenation, and enhanced burial of organic matter) and the secular

evolution of atmospheric O_2 levels. In contrast, these scenarios demonstrate different climatic variations. Specifically, the enhanced terrestrial nutrient export scenarios suggest a marked decrease in atmospheric CO_2 and global cooling of >1°C whereas the enhanced volcanic activity results in the two-fold increase in atmospheric CO_2 levels and global warming of >4°C. Additionally, while both scenarios achieve the positive $d^{13}C$ excursion recorded in the geologic record, the longevity of the excursions in the enhanced volcanic activity scenario tends to be longer than those of the terrestrial nutrient export scenarios because of the increased residence time of inorganic carbon in the ocean-atmosphere system. Additionally, maxima in climate cooling in the enhanced terrestrial nutrient export scenario correspond to the largest positive excursion in $d^{13}C$, whereas in the enhanced volcanic activity scenario, the $d^{13}C$ excursion is delayed and occurs after the temperature maxima.

Both scenarios are somewhat at odds with the geologic record in differing respects. While an overall warming trend is observed through the End Devonian, conodont oxygen isotope records from numerous studies suggest cooling leading into both the LKW and UKW[6,14,43,44]. If large scale volcanism (either from LIP or multiple arc volcanic events[20]) was an initiating event, the enhanced volcanic activity scenario requires warming on a global scale (Fig. 4f) which is not universally supported by conodont oxygen isotope records. Additionally, atmospheric CO_2 decreased substantially throughout the Devonian. Our model predicts large scale volcanism sufficient to drive anoxia would have increased atmospheric CO_2 to levels which are likewise not supported in the geologic record. A compilation published by Franks et al.[29] compares Paleozoic CO_2 estimates from paleosol carbonates, fossil records and model estimates using GEOCARBSULF and reports a likely atmospheric CO_2 range of between 500-3000 ppm for the Late Devonian, substantially below >20 PAL required by our model (see also[30,31]). However, many of these records lack the temporal resolution to detect short-time scale perturbations, so although current evidence does not support rapid and dramatic increases in atmospheric CO_2 due to large scale volcanism it cannot be completely ruled out.

Our model results are most consistent with enhanced terrestrial nutrient export as an important causal factor in at least the UKW extinction pulse as the predicted cooling, decrease in atmospheric CO_2, and increase in atmospheric O_2 are all supported by the geologic record. The P/Al based model predicts larger geochemical perturbations during the LKW, which is inconsistent with most records that suggest the UKW was the more significant. This contrasts with phosphorus accumulation rate-based data which accurately predicts the UKW as the more significant event. Additionally, the similarities in geochemical response between the Heintzbjerg sequence and the linear simulations further reinforce the supposition that the terrestrial nutrient export model is the more likely of the two scenarios. However, the timing of the terrestrial nutrient pulses[26] seems to preclude plant expansion as an initiating event. Although there is evidence of elevated nutrient export during the LKW and at the start of the UKW, the most significant and sustained nutrient export event occurs in the second half of the UKW, closer to the Frasnian-Famennian boundary (Fig. 2). While land plants may not have directly initiated the UKW, the concurrent extinction of both benthic species and the collapse of Devonian Reefs systems suggest the possibility of multiple

extinction mechanisms. Rather than singular triggers, we suggest multiple elements of current theories contributed to biotic crises in the marine biosphere.

A Multifaceted Extinction Mechanism

The Heintzbjerg sequence is a terrestrial equivalent to marine expressions of the KW events and is characterized by the deposition of two intervals of thick sandstones representing intense fluvial activity followed by stacks of palaeosols representing intense and prolonged intervals of aridity (see Fig. 2)[45]. These sedimentary markers suggest that the deposition of the UKW horizon at Heintzbjerg marks a defined shift in climate regimes from arid to warm and wet[26,45]. Concurrent with this shift in climatic regimes is evidence of elevated terrestrial phosphorus export (Fig. 2). Such a climate shift would bring about conditions generally more favorable for plant growth, potentially explaining enhanced terrestrial phosphorus export at the start of the UKW. Additionally, at least one pulse of both the Viluy and Pripyat-Dnieper-Donets (PDD) LIPs (the largest Devonian LIPs and the two most closely associated temporally with the KW events) occurred during the UKW[21,47]. While our model predictions appear to rule out cataclysmic volcanism as a sole extinction mechanism, they do not discount it completely.

At the onset of the UKW, our model predicts substantial geochemical changes with increased terrestrial nutrient delivery driving positive $\delta^{13}C$ excursions, corresponding increases in O_2 and DOA and significant decreases in CO_2 and temperature. One possibility suggested by the model data is that a significant volcanic event increased atmospheric CO_2 prior to the UKW, but was insufficient in magnitude to drive extinction on its own. A high CO_2 environment catalyzed by large scale volcanism combined with a climatic shift to wetter conditions at the UKW onset would drive increased rates of silicate rock weathering, increase carbon sequestration and eventually draw down atmospheric CO_2. Additionally, high atmospheric CO_2 would create a favorable environment for plant growth (i.e., the CO_2 fertilization effect[48]). Indeed, our model predicts an increase in net primary production (NPP) on land for the enhanced volcanic degassing scenario accompanying both the LKW and UKW extinction pulses on the order of 2.5 and 6.2 Gt C yr^{-1} for each, respectively (Extended Data Fig. 1). Combined with a warm and wet climate, a large but transitory increase in atmospheric CO_2 may have been sufficient to sustain a rapid expansion of land plants in the late Frasnian, resulting in the observed massive terrestrial export of phosphorus[26]. This phosphorus would have made its way to the Rheic Ocean, driving anoxia not only in the deeper portions of the basin, but also eutrophication of the shallower margins, partially explaining the decimation of Devonian reef systems observed at the Frasnian-Famennian boundary. Plant expansion tied to transitory increases in atmospheric CO_2 concentrations and climatic shifts has previously been proposed as an explanation for the staggered expansion of land plants in Mid Devonian New York, USA[46] and appears possible in the Devonian Basin in East Greenland as well[26]. Our model, supported by geochemical data, suggests that climatic changes possibly in concert with large scale volcanism encouraged plant expansion in East Greenland. The geochemical instability initiated by large scale volcanism combined with the rapid geochemical feedbacks produced by the collective effects of

increased rates of silicate rock weathering and land plant expansion would have been sufficient to drive widespread ocean anoxia culminating in mass extinction.

Extinction events are complex systemic responses, and with rare exceptions have seldom been attributed to a single cataclysm. The various theories regarding the initiation of the KW events may each be correct in that they likely contributed to the ecological crisis, although their true timing and sequence clearly need refinement. Our results suggest that neither large scale volcanism nor land plant evolution can be implicated as the sole initiating factor in the KW event. Instead, the KW event was the timely combination of multiple events ultimately resulting in the decimation of Devonian seas. Evidence presented here challenges a single extinction mechanism and demonstrates the need for further work integrating multiple theories to bring together the exact timing and sequence of events which culminated in one of the Phanerozoic's most significant mass extinctions.

Methods

P/Al and Phosphorus Accumulation Data

P/Al data was taken directly from[26] (Fig. 2) and scaled as described below. Due to limitations in the sample repository at the University of Southampton from which the Heintzbjerg samples were sourced, the initiation of the LKW was not covered in the Heintzbjerg sample set and thus, [26] were unable to establish an age control point at the base of the LKW (nor were they able to establish an age control point for the significant number of samples in the Famennian). Age control points were available for the end of the LKW, base of the UKW and the Frasnian-Famennian boundary and were used to calculate average sedimentation rates and phosphorus (P) accumulation rates between each of those sections[26]. Although the P/Al data is informative of terrestrial phosphorus export, P accumulation rate is a more robust parameter from which to gauge phosphorus weathering by land plants and subsequent landscape stabilization (see[26,49,50]). In order to use P accumulation data as an input into our model however, it was critical that sedimentation rates, and thus P accumulation rates, be calculated for the entire sequence to capture not only the LKW, but also the post-UKW geochemical response.

Recent refinements in the age of the Frasnian-Famennian boundary from similar sequences[16,27] make it possible to use relative dating techniques to established estimated ages for the entire sequence based on this anchor point, thus allowing calculation of sedimentation rates and P accumulation rates for the entire Heintzbjerg sequence. The field of astrochronology has long used Milankovitch cycles to gauge the passage of time in sedimentary sequences. Climatic oscillations recorded in the sedimentary record can be tied to changes in the Earth's orbital parameters. Specifically, the ellipticity of Earth's orbit (referred to as eccentricity, with periods of 405 kyr, 123 kyr and 95 kyr), tilt (referred to as obliquity, with a modern period of 41 kyr and varying periods in deep time[51]) and precession (with a modern period of 20 kyr and also varying in deep time[51]). Meyers[52] (further refined in[53]) utilized a statistical optimization method called TimeOpt in the *Astrochron* package in the R platform[54] in order to correlate climatic changes in the stratigraphic record with Milankovitch cycles to establish relative age of a sedimentary sequence. We

employ a similar approach here, but utilize the timeOptTemplate function which was designed for more complex sedimentation models[53] which we expected to encounter given the wet/arid climatic shifts noted in the Heintzbjerg sedimentary sequence. The timeOptTemplate function allows the use of proxy or lithology-specific templates which greatly enhance the spectral alignment and overall fit for complex sedimentary sequences. We evaluated the utility of multiple climate-related proxies using this method along with geochemical data from[26] ultimately selecting Rb/Sr and Log Ti as proxies which produced the best spectral alignment and overall fit (e.g., [16]). Eccentricity periods of 94.9, 98.9, 123.8, 130.7 and 405 kyr[55] along with precession periodicities for the Devonian of 16.85 and 19.95 kyr[51] were utilized. The sedimentation rates estimated using timeOptTemplate were compared with sections calculated by[26] and found to be of similar magnitude (Midnatspas average sedimentation rate = 43 cm kyr^{-1} (see [26]) compared with 71.9 cm kyr^{-1} (timeOptTemplate); UKW average sedimentation rate = 272 cm kyr^{-1} (see [26]) compared with 228.6 cm kyr^{-1} (timeOptTemplate). Age estimates were then determined based on the Frasnian-Famennian boundary (371.870 Ma[16]) as an anchor point and compared with age estimates for similar published sequences[16,27]. Using timeOptTemplate estimations, we calculated the base of the UKW of our sequence at 372.06 Ma (compared with 372.00 − 372.02 Ma based on[16,27]) and the end of the LKW at 372.49 Ma (compared with 372.45 Ma based on[16]), a mere 40 kyr difference for each and lending confidence in the validity of the timeOptTemplate results.

Based on the relative confirmation of the timeOptTemplate results, new P accumulation rates were calculated for the entire Heintzbjerg sequence. Once again, these results were compared with those sections calculated in[26] and found to be strikingly similar in overall trends, but notably with somewhat differing magnitudes (Extended Data Fig. 2). The differences in magnitude however, do not change the overall interpretation by[26]. Thus, these new P accumulation rates were used as input into our model as described below.

Earth system box model

The basic model design in this study was based on the Carbon Oxygen Phosphorus Sulfur Evolution (COPSE) model[41,42], which has been extensively tested and validated against geologic records during the Phanerozoic. We incorporate refinements to this model from Ozaki and Reinhard[40] and extend the biogeochemical framework for the global methane (CH_4) cycle without altering the basic behavior of the model. While Ozaki and Reinhard[40] include the mass exchange between the surface system (atmosphere-ocean-crust) and the mantle, we ignore this in this study. We initialized the model at 600 Ma and ran the model forward in time until the end Famennian. Specific model parameters for each experiment are outlined in the following two sections.

Enhanced terrestrial nutrient export model

To test the enhanced P export hypothesis, we introduced a forcing factor, f_{pP}, which represents the amplification factor for the terrestrial phosphorus weathering flux:

$$J_P^w = f_{pP} \left(\frac{2}{12} \frac{J_{sil}^w}{J_{sil}^{w,*}} + \frac{5}{12} \frac{J_{carb}^w}{J_{carb}^{w,*}} + \frac{5}{12} \frac{J_{orgC}^w}{J_{orgC}^{w,*}} \right) J_P^{w,*},$$ (1)

where J_P^w, J_{sil}^w, J_{carb}^w, and J_{org}^w denote the rates of phosphorus weathering, silicate weathering, carbonate weathering, and the oxidative weathering of organic matter on land, respectively, and * represents the reference value (pre-industrial flux; see[40,41]). To assess the uncertainty in the timing and amplitude of pulses in phosphorus weathering, we explored the following different scenarios: (i) In an attempt to reproduce the 2-3‰ positive excursions in d^{13}C, the following forcing factors were assumed; (LKW) f_{pP} = 1→2→1 over 372.72-372.54-372.36 Ma. (UKW) f_{pP} = 1→2→1 over 372.1-371.91-371.73 Ma. (ii) As i but decreasing the forcing factor to 1.5 for both the LKW and UKW. (iii) As i but decreasing the forcing factor to 1.5 for the LKW only. (iv) f_{pP} based on the P/Al data from Heintzbjerg, Greenland (Fig. 3, left panel), with a scaling factor of 0.5 (see below). (v) f_{pP} based on P accumulation data from Heintzbjerg (Fig. 3, right panel) and applying a scaling factor of 0.15 to account for the hypothesized episodic expansion of land plants as predicted by[26,46], assuming a maximum value of f_{pP} = 3.35.

To convert the sedimentary data of P (P/Al or P accumulation rate) into the forcing factor of f_{pP} in (iv) and (v), we first calculate the typical 'non-event' value by averaging data between LKW and UKW (Midnatspas Fm.), X_{avg}. Then, f_{pP} is calculated, as follows:

$$f_{pP} = 1 + \frac{X - X_{avg}}{X_{avg}} a,$$ (2)

where X denotes the sedimentary data of P (P/Al or P accumulation rate) and a represents the scaling factor. When a = 1, f_{pP} (and global P loading flux) simply reflects the variation of P flux observed at Heintzbjerg. But, in this case, our model predicts an extremely large positive excursion of d^{13}C (10‰), inconsistent with geologic records. The scaling factor is therefore introduced to represent the relationship between the Heintzbjerg P records to global P export flux. The value of a was tuned so that the model produces a reasonable positive excursion of d^{13}C of 2-3‰.

Enhanced volcanic activity model

To understand the biogeochemical consequences of the enhanced volcanic activity, we introduced a forcing factor, f_{LIP}, which is multiplied by the degassing rate of CO_2 via carbonate and organic carbon metamorphisms:

$$J_{carb}^{m} = f_{LIP} f_{G} f_{C} \left(\frac{C}{C^{*}} \right) J_{carb}^{m,*}, \qquad (3)$$

$$J_{org}^{m} = f_{LIP} f_{G} \left(\frac{G}{G^{*}} \right) J_{org}^{m,*} \qquad (4)$$

where J_{carb}^{m} and J_{org}^{m} denote carbon dioxide (CO_2) degassing flux via metamorphism of sedimentary carbonate (C) and organic carbon (G), respectively (* represent reference values found in[41]). f_{G} and f_{C} represent the forcing factors of degassing flux and pelagic carbonate deposition which are used in the original model. By varying the value of f_{LIP}, we explore the possible impacts of CO_2 degassing rate on global biogeochemistry (Fig. 4): f_{LIP} = 1→2→1 over 372.72-372.54-372.36 Ma. (UKW) f_{LIP} = 1→5→1 over 372.1-371.91-371.73 Ma.

Declarations

Author contributions

MSS, GF and WPG designed the study. CTR and KO designed the mathematical model and KO ran the model. MSS and KO interpreted the data. GF, WPG, JHW and JEAM assisted with interpretations. MSS wrote the manuscript with significant input from KO. MSS, GF, WPG, CTR and KO reviewed the manuscript.

Competing interests

The authors declare no competing interests.

Data availability

The datasets generated during and/or analyzed during the current study are available from the corresponding author on reasonable request.

References

1. Raup, D. M., & Sepkoski, J. J. (1982). Mass extinctions in the marine fossil record. *Science*, 215(4539), 1501-1503.

2. McGhee Jr, G. R., Clapham, M. E., Sheehan, P. M., Bottjer, D. J., & Droser, M. L. (2013). A new ecological-severity ranking of major Phanerozoic biodiversity crises. *Palaeogeography, Palaeoclimatology, Palaeoecology*, 370, 260-270.

3. Bond, D., Wignall, P. B., & Racki, G. (2004). Extent and duration of marine anoxia during the Frasnian–Famennian (Late Devonian) mass extinction in Poland, Germany, Austria and France. *Geological Magazine*, 141(2), 173-193.

4. Carmichael, S. K., Waters, J. A., Koenigshof, P., Suttner, T. J., & Kido, E. (2019). Paleogeography and paleoenvironments of the Late Devonian Kellwasser event: A review of its sedimentological and geochemical expression. *Global and Planetary Change*, 183, 102984.

5. Joachimski, M. M., & Buggisch, W. (1993). Anoxic events in the late Frasnian—Causes of the Frasnian-Famennian faunal crisis? *Geology*, 21(8), 675-678.

6. Joachimski, M. M., & Buggisch, W. (2002). Conodont apatite δ18O signatures indicate climatic cooling as a trigger of the Late Devonian mass extinction. *Geology*, 30(8), 711-714.

7. Chen, D., Qing, H., & Li, R. (2005). The Late Devonian Frasnian–Famennian (F/F) biotic crisis: insights from δ13Ccarb, δ13Corg and 87Sr/86Sr isotopic systematics. Earth and *Planetary Science Letters*, 235(1-2), 151-166.

8. House, M. R. (1985). Correlation of mid-Palaeozoic ammonoid evolutionary events with global sedimentary perturbations. *Nature*, 313(5997), 17-22.

9. Buggisch, W. (1991). The global Frasnian-Famennian Kellwasser Event. *Geologische Rundschau*, 80(1), 49-72.

10. Bond, D. P., Zatoń, M., Wignall, P. B., & Marynowski, L. (2013). Evidence for shallow-water 'Upper Kellwasser'anoxia in the Frasnian–Famennian reefs of Alberta, Canada. *Lethaia*, 46(3), 355-368.

11. Thompson, J. B., & Newton, C. R. (1988). Late Devonian mass extinction: episodic climatic cooling or warming? Paleontology, *Paleoecology and Biostratigraphy,* Proceedings of the 2nd International Symposium on the Devonian System — Memoir 14, 3, 29-34.

12. Joachimski, M. M., Pancost, R. D., Freeman, K. H., Ostertag-Henning, C., & Buggisch, W. (2002). Carbon isotope geochemistry of the Frasnian–Famennian transition. *Palaeogeography, Palaeoclimatology, Palaeoecology*, 181(1-3), 91-109.

13. Xu, B., Gu, Z., Wang, C., Hao, Q., Han, J., Liu, Q., ... & Lu, Y. (2012). Carbon isotopic evidence for the associations of decreasing atmospheric CO2level with the Frasnian-Famennian mass extinction. Journal of Geophysical Research: *Biogeosciences*, 117(G1).

14. Huang, C., Joachimski, M. M., & Gong, Y. (2018). Did climate changes trigger the Late Devonian Kellwasser Crisis? Evidence from a high-resolution conodont δ18OPO4 record from South China. *Earth and Planetary Science Letters*, 495, 174-184.

15. Wang, X., Liu, S. A., Wang, Z., Chen, D., & Zhang, L. (2018). Zinc and strontium isotope evidence for climate cooling and constraints on the Frasnian-Famennian (~ 372 Ma) mass extinction.

Palaeogeography, Palaeoclimatology, Palaeoecology, 498, 68-82.

16. Da Silva, A. C., Sinnesael, M., Claeys, P., Davies, J. H., de Winter, N. J., Percival, L. M. E., ... & De Vleeschouwer, D. (2020). Anchoring the Late Devonian mass extinction in absolute time by integrating climatic controls and radio-isotopic dating. *Scientific Reports*, 10(1), 1-12.

17. Lu, M., Lu, Y., Ikejiri, T., Sun, D., Carroll, R., Blair, E. H., ... & Sun, Y. (2021). Periodic oceanic euxinia and terrestrial fluxes linked to astronomical forcing during the Late Devonian Frasnian–Famennian mass extinction. *Earth and Planetary Science Letters*, 562, 116839.

18. Claeys, P., Casier, J. G., & Margolis, S. V. (1992). Microtektites and mass extinctions: evidence for a Late Devonian asteroid impact. Science, 257(5073), 1102-1104.

19. McGhee Jr, G. R. (2001). The 'multiple impacts hypothesis' for mass extinction: a comparison of the Late Devonian and the late Eocene. *Palaeogeography, Palaeoclimatology, Palaeoecology*, 176(1-4), 47-58.

20. Racki, G., Rakociński, M., Marynowski, L., & Wignall, P. B. (2018). Mercury enrichments and the Frasnian-Famennian biotic crisis: A volcanic trigger proved? *Geology*, 46(6), 543-546.

21. Racki, G. (2020). A volcanic scenario for the Frasnian–Famennian major biotic crisis and other Late Devonian global changes: More answers than questions? *Global and Planetary Change*, 189, 103174.

22. Averbuch, O., Tribovillard, N., Devleeschouwer, X., Riquier, L., Mistiaen, B., & Van Vliet-Lanoe, B. (2005). Mountain building-enhanced continental weathering and organic carbon burial as major causes for climatic cooling at the Frasnian–Famennian boundary (c. 376 Ma)? *Terra Nova*, 17(1), 25-34.

23. Percival, L. M. E., Selby, D., Bond, D. P. G., Rakociński, M., Racki, G., Marynowski, L., ... & Föllmi, K. B. (2019). Pulses of enhanced continental weathering associated with multiple Late Devonian climate perturbations: Evidence from osmium-isotope compositions. *Palaeogeography, Palaeoclimatology, Palaeoecology*, 524, 240-249.

24. Algeo, T. J., Berner, R. A., Maynard, J. B., & Scheckler, S. E. (1995). Late Devonian oceanic anoxic events and biotic crises: "rooted" in the evolution of vascular land plants. *GSA Today*, 5(3), 45-66.

25. Algeo, T. J., & Scheckler, S. E. (1998). Terrestrial-marine teleconnections in the Devonian: links between the evolution of land plants, weathering processes, and marine anoxic events. Philosophical Transactions of the Royal Society of London. Series B: *Biological Sciences*, 353(1365), 113-130.

26. Smart, M. S., Filippelli, G. M., Gilhooly, W.P., Marshall, J.E.A. & Whiteside, J. H., (2022). Enhanced terrestrial nutrient release during the Devonian emergence and expansion of forests: Evidence from lacustrine phosphorus and geochemical records. *GSA Bulletin*. In press.

27. Percival, L. M. E., Bond, D. P. G., Rakociński, M., Marynowski, L., Hood, A. V. S., et al. (2020). Phosphorus-cycle disturbances during the Late Devonian anoxic events. *Global andPplanetary Change*, 184, 103070.

28. Royer, D. L., Berner, R. A., & Park, J. (2007). Climate sensitivity constrained by CO2 concentrations over the past 420 million years. *Nature*, 446(7135), 530-532.

29. Franks, P. J., Royer, D. L., Beerling, D. J., Van de Water, P. K., Cantrill, D. J., et al.. (2014). New constraints on atmospheric CO2 concentration for the Phanerozoic. *Geophysical Research Letters*, 41(13), 4685-4694.

30. Royer, D. L. (2014). Atmospheric CO2 and O2 during the Phanerozoic: Tools, patterns, and impacts. *Treatise on Geochemistry* (Second Edition), 6.

31. Lenton, T. M., Daines, S. J., & Mills, B. J. (2018). COPSE reloaded: an improved model of biogeochemical cycling over Phanerozoic time. Earth-Science Reviews, 178, 1-28.

32. Algeo, T. J., & Ingall, E. (2007). Sedimentary Corg: P ratios, paleocean ventilation, and Phanerozoic atmospheric pO2. *Palaeogeography, Palaeoclimatology, Palaeoecology*, 256(3-4), 130-155.

33. Berner, R. A. (2009). Phanerozoic atmospheric oxygen: New results using the GEOCARBSULF model. *American Journal of Science*, 309(7), 603-606.

34. Zhang, L., Chen, D., Huang, T., Yu, H., Zhou, X., et al. (2020). An abrupt oceanic change and frequent climate fluctuations across the Frasnian−Famennian transition of Late Devonian: constraints from conodont Sr isotope. *Geological Journal*, 55(6), 4479-4492.

35. Scotese, C. R., Song, H., Mills, B. J., & van der Meer, D. G. (2021). Phanerozoic paleotemperatures: The earth's changing climate during the last 540 million years. *Earth-Science Reviews*, 103503.

36. Scotese, C. R. (2016). Tutorial: PALEOMAP paleoAtlas for GPlates and the paleoData plotter program.

37. Meyer-Berthaud, B., Scheckler, S. E., & Wendt, J. (1999). Archaeopteris is the earliest known modern tree. *Nature*, 398(6729), 700-701.

38. Meyer-Berthaud, B., Soria, A., & Decombeix, A. L. (2010). The land plant cover in the Devonian: a reassessment of the tree habit. *Geological Society*, London, Special Publications, 339(1), 59-70.

39. Stein, W. E., Berry, C. M., Morris, J. L., Hernick, L. V., Mannolini, F., et al. (2020). Mid-Devonian Archaeopteris roots signal revolutionary change in earliest fossil forests. , 30(3), 421-431.

40. Ozaki, K., Reinhard, C.T., 2021. The future lifespan of Earth's oxygenated atmosphere. *Nature Geoscience*. 14, 138-142.

41. Bergman, N.M., Lenton, T.M., Watson, A.J., 2004. COPSE: A new model of biogeochemical cycling over Phanerozoic time. *American Journal of Science*. 304, 397-437.

42. Lenton, T.M., Dahl, T.W., Daines, S.J., Mills, B.J.W., Ozaki, K., Saltzman, M.R., Porada, P, 2016. Earliest land plants created modern levels of atmospheric oxygen. *Proceedings of the National Academy of Sciences*. USA 113, 9704-9709.

43. Balter, V., Renaud, S., Girard, C., & Joachimski, M. M. (2008). Record of climate-driven morphological changes in 376 Ma Devonian fossils. *Geology*, 36(11), 907-910.

44. Joachimski, M. M., Breisig, S., Buggisch, W., Talent, J. A., Mawson, R., et al. (2009). Devonian climate and reef evolution: insights from oxygen isotopes in apatite. *Earth and Planetary Science Letters*, 284(3-4), 599-609.

45. Larsen, P. H., Olsen, H., & Clack, J. A. (2008). The Devonian basin in East Greenland—Review of basin evolution and vertebrate assemblages. The Greenland Caledonides: Evolution of the Northeast Margin of Laurentia: *Geological Society of America Memoir*, 202, 273-292.

46. Retallack, G. J., & Huang, C. (2011). Ecology and evolution of Devonian trees in New York, USA. *Palaeogeography, Palaeoclimatology, Palaeoecology*, *299*(1-2), 110-128.

47. Ernst, R. E., Rodygin, S. A., & Grinev, O. M. (2020). Age correlation of Large Igneous Provinces with Devonian biotic crises. *Global and Planetary Change*, 185, 103097.

48. Ueyama, M., Ichii, K., Kobayashi, H., Kumagai, T. O., Beringer, J., et al. (2020). Inferring CO2 fertilization effect based on global monitoring land-atmosphere exchange with a theoretical model. *Environmental Research Letters*, 15(8), 084009.

49. Filippelli, G.M., and Souch, C., 1999, Effects of climate and landscape development on the terrestrial phosphorus cycle: Geology, v. 27, p. 171.

50. Filippelli, G.M., 2002, The Global Phosphorus Cycle: *Reviews in Mineralogy and Geochemistry*, v. 48, p. 391–425.

51. Berger, A., Loutre, M. F., & Laskar, J. (1992). Stability of the astronomical frequencies over the Earth's history for paleoclimate studies. *Science*, 255(5044), 560-566.

52. Meyers, S. R. (2015). The evaluation of eccentricity‚Äêrelated amplitude modulation and bundling in paleoclimate data: An inverse approach for astrochronologic testing and time scale optimization. *Paleoceanography*, 30(12), 1625-1640.

53. Meyers, S. R. (2019). Cyclostratigraphy and the problem of astrochronologic testing. *Earth-Science Reviews*, 190, 190-223.

54. Core Team, R. R: A language and environment for computing (2022).

55. Laskar, J., Fienga, A., Gastineau, M., & Manche, H. (2011). La2010: a new orbital solution for the long-term motion of the Earth. *Astronomy & Astrophysics*, 532, A89.

56. Filippelli, G. M. (1997). Controls on phosphorus concentration and accumulation in oceanic sediments. *Marine Geology*, 139(1-4), 231-240.
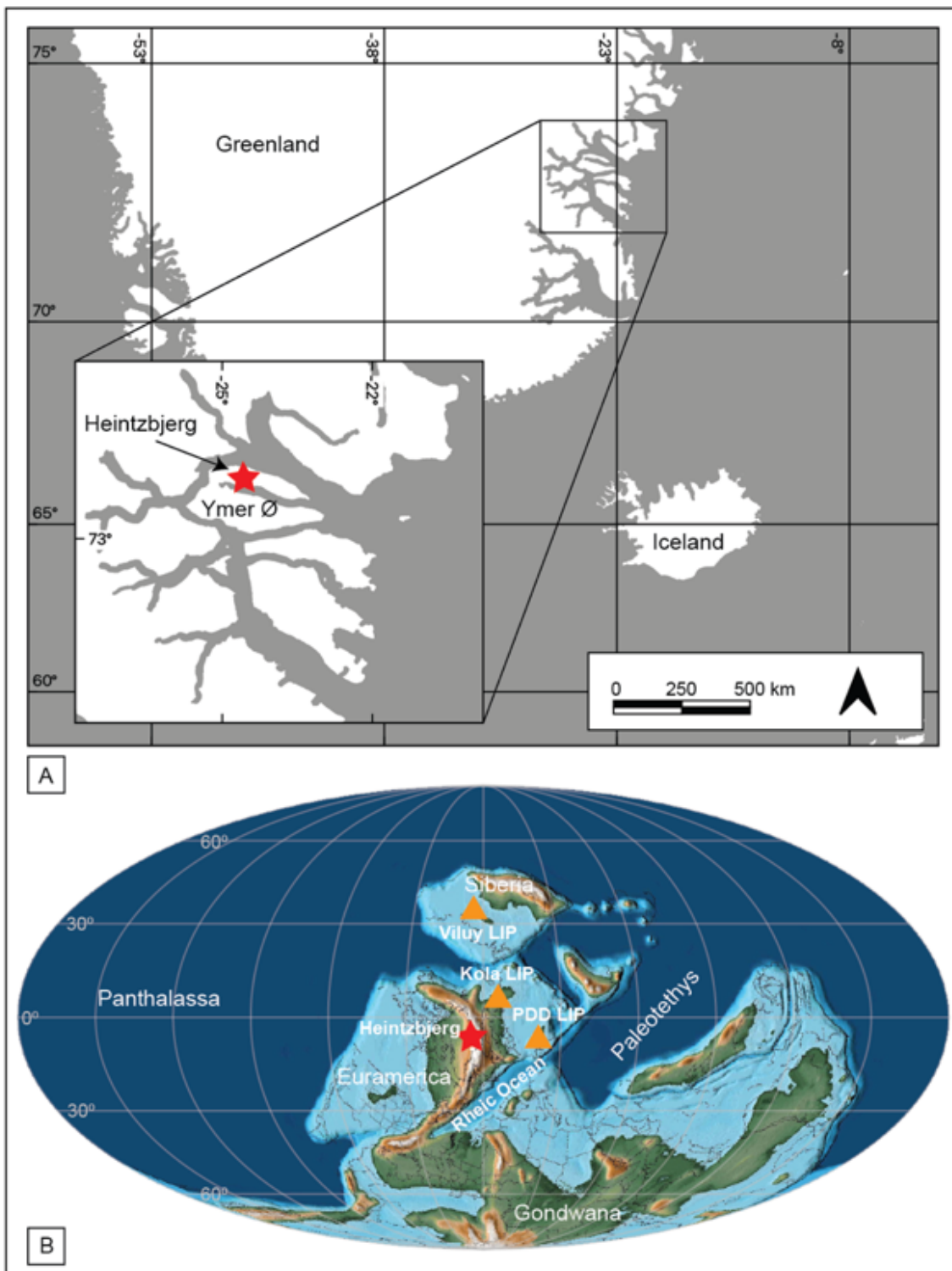
Figures

Figure 1

A. Location of the study site from which model data is derived (indicated by a star). B. Late Devonian (~370 Ma) paleogeographic reconstruction with the study location indicated by a star as well as the relative locations of significant Late Devonian large igneous provinces (LIPs) indicated by triangles. Significant LIPs include the Viluy LIP in Siberia, the Kola LIP in the Kola Peninsula and the Pripyat-

Dnieper-Donets (PDD) LIP in East Europe. The base map was created using GPlates with reconstructions from[36]. Locations of LIPs as described by[21].
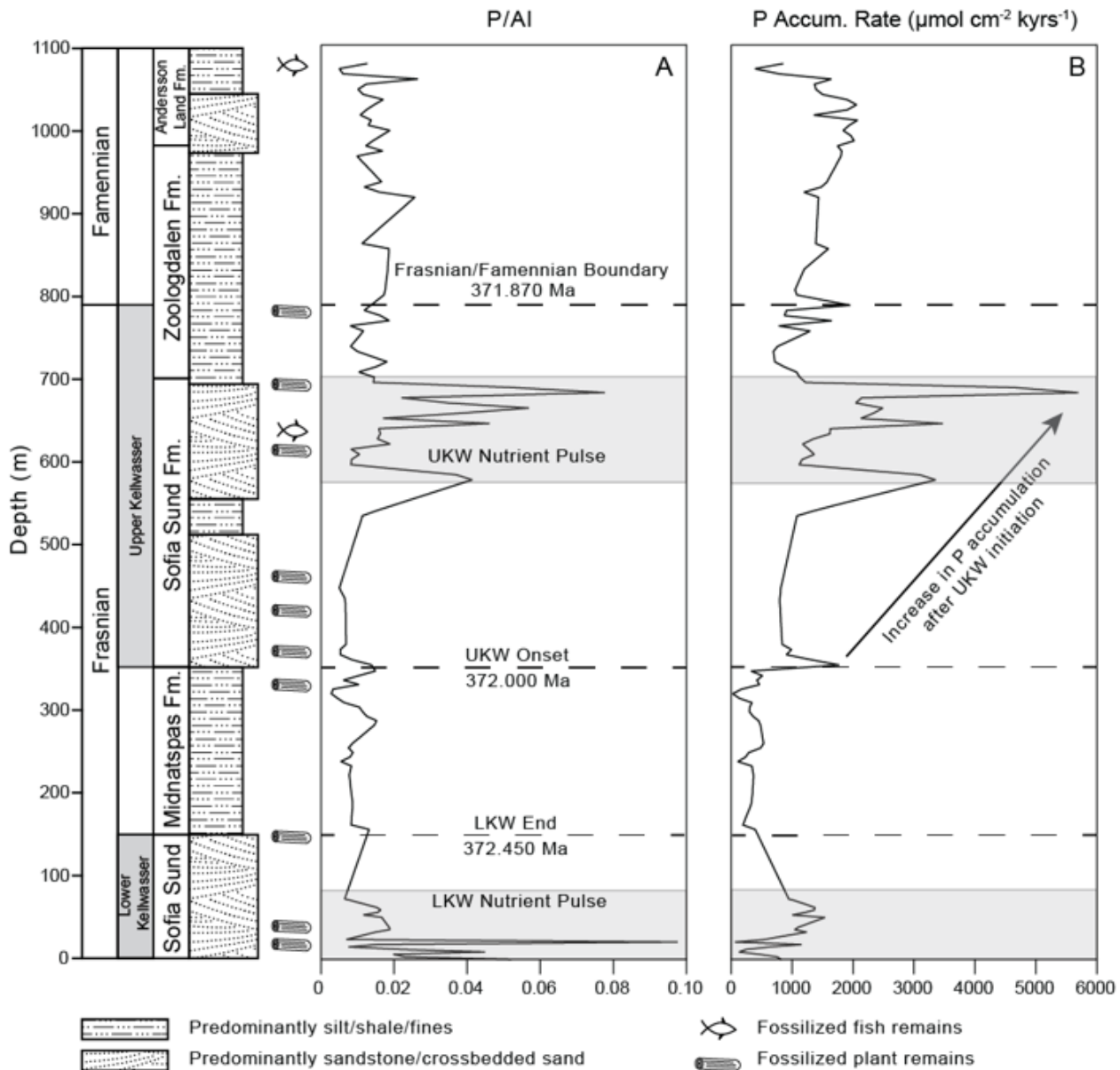

Figure 2

Geochemical source data from the study location[26]. The Heintzbjerg sequence contains 1100 m of continuous fluvial record capturing a portion of the Lower Kellwasser (LKW) as well as the entirety of the Upper Kellwasser (UKW) events comprising the Frasnian-Famennian extinction. Stratigraphy has been simplified due to the size of the sequence. Black dashed lines represent the age control points used to calculate sedimentation rates based on recent age estimates[16,27]. Shaded regions represent nutrient pulses during the LKW and UKW based on P/Al data[26]. A. Phosphorus/aluminum ratios used to estimate riverine phosphorus flux. Based on this data, two distinct nutrient pulses can be identified. B. Phosphorus

accumulation rate data calculated using estimated sedimentation rates based on cyclostratigraphy and used to simulate terrestrial phosphorus input in a separate simulation. These data show a greatly reduced nutrient pulse during the LKW and a large and sustained nutrient pulse during the UKW.
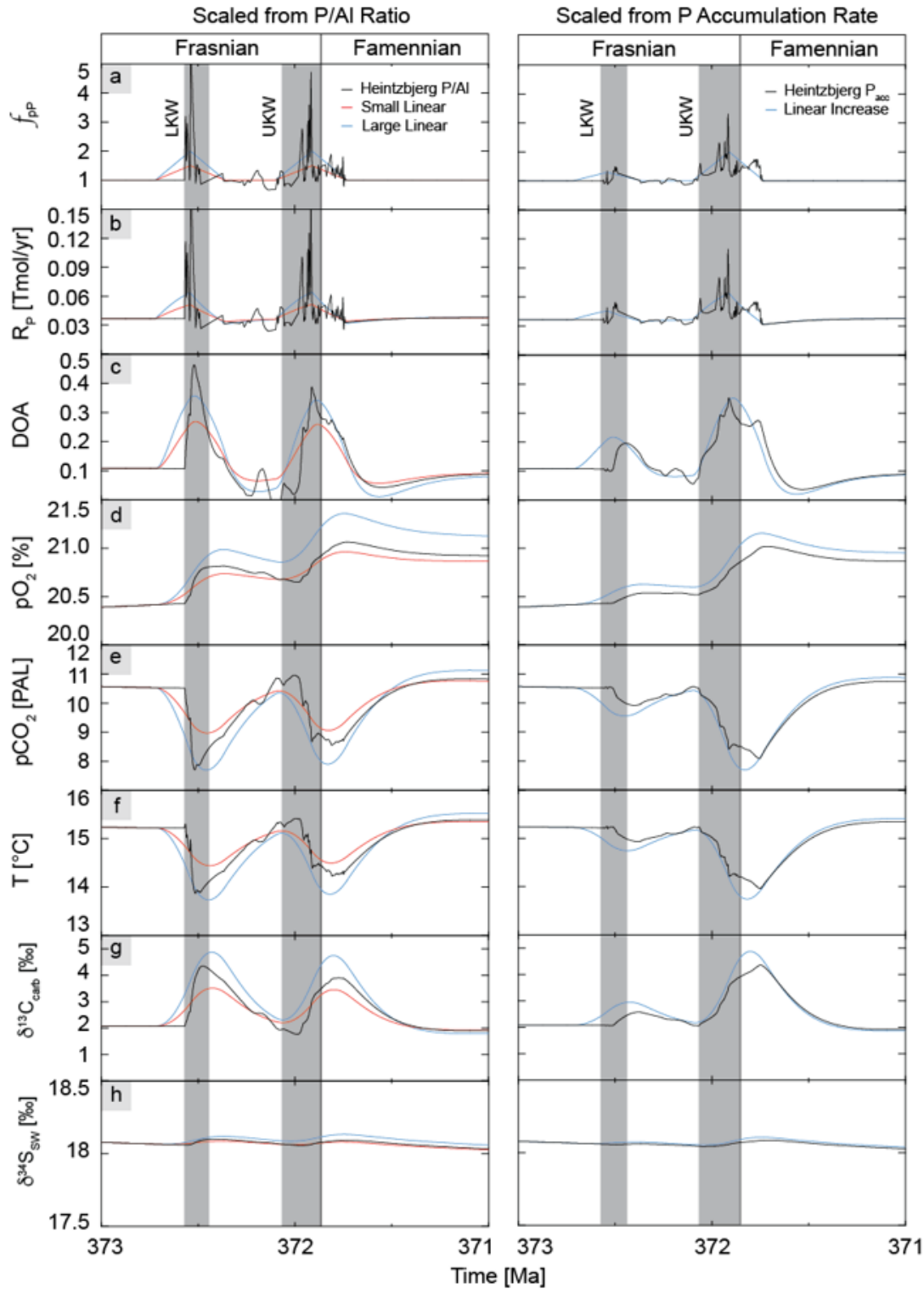

Figure 3

Biogeochemical dynamics induced by elevated episodes of P weathering on land. Gray shaded regions represent the two pulses of the Kellwasser extinction. (a) Phosphorus weathering forcing factor, f_{pP}. Several different scenarios are explored: red and blue lines assume episodes with linear increase and decrease around the LKW and UKW, and black line is obtained by scaling the P/Al (left panel) and phosphorus accumulation rate (right panel) records from Heintzbjerg, Greenland. (b) Riverine P flux to the ocean. (c) Degree of oceanic anoxia. (d) Atmospheric O_2 level. (e) Atmospheric CO_2 level. PAL = present atmospheric level. (f) Global average surface temperature. (g) Carbon isotopic value of burying carbonates. (h) Seawater sulfate sulfur isotope.
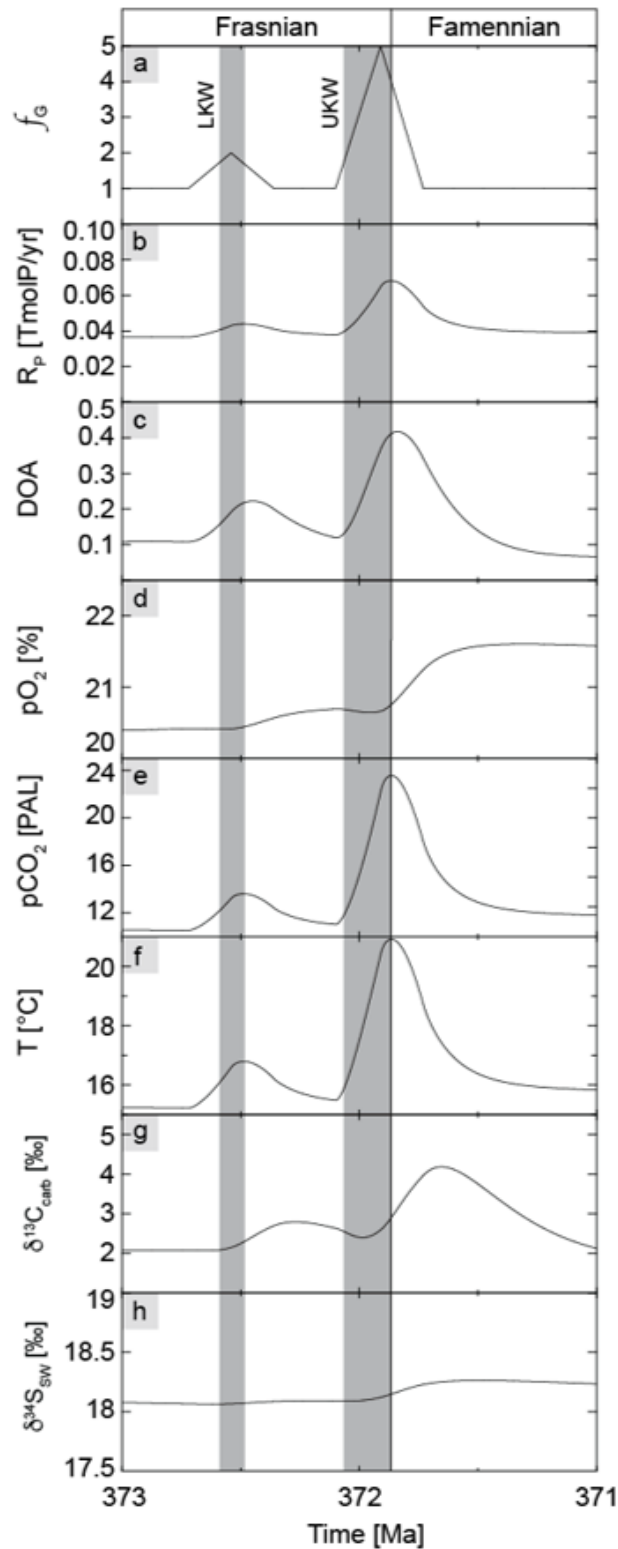
Figure 4

Biogeochemical dynamics induced by enhanced volcanic activity. Black line represents two distinct volcanic events, one during the LKW and a second during the UKW based on the presence of two distinct weathering events in the Heintzbjerg, Greenland data. Gray shaded region represents the two pulses of the Kellwasser extinction. (a) Degassing factor, f_G. (b) Riverine P flux to the ocean. (c) Degree of anoxia.

(d) Atmospheric O_2 level. (e) Atmospheric CO_2 level. PAL = present atmospheric level. (f) Global average surface temperature. (g) Carbon isotopic value of burying carbonates. (h) Seawater sulfate sulfur isotope.

Supplementary Files

This is a list of supplementary files associated with this preprint. Click to download.

- ExtendedData.docx